Science of the Total Environment 806 (2022) 150530

Contents lists available at ScienceDirect

Science of the Total Environment

journal homepage: www.elsevier.com/locate/scitotenv

Spatio-temporal variation of microplastic pollution in the sediment from the Chukchi Sea over five years

Chao Fang [a], Yusheng Zhang [a], Ronghui Zheng [a], Fukun Hong [a], Min Zhang [a], Ran Zhang [a], Jianfeng Mou [a], Jingli Mu [b], Longshan Lin [a,*], Jun Bo [a,*]

[a] Laboratory of Marine Biology and Ecology, Third Institute of Oceanography, Ministry of Natural Resources, Xiamen 361102, China
[b] Fujian Key Laboratory of Functional Marine Sensing Materials, Institute of Oceanography, Minjiang University, Fuzhou 350108, China

HIGHLIGHTS

- MP abundance in the sediment from Chukchi Plateau exhibited an increasing trend.
- The Chukchi Plateau is a hotspot for MPs related to fishing gear and textiles.
- The receding sea ice in the Chukchi Sea promoted the increase in sedimentary MPs.
- Blue and smaller MPs increased in the sediment from the Chukchi Plateau.
- Chukchi Shelf might be a source of some engineering-and industry-related MPs.

GRAPHICAL ABSTRACT

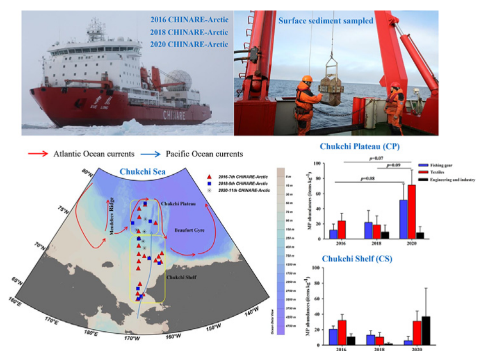

ARTICLE INFO

Article history:
Received 3 August 2021
Received in revised form 14 September 2021
Accepted 19 September 2021
Available online 24 September 2021

Editor: Dimitra A Lambropoulou

Keywords:
Arctic
Sediment
Western Arctic Ocean
Chukchi Plateau
Sea ice
Microplastic

ABSTRACT

Sediment has been considered as an important sink for microplastics (MPs), but there are limited reports about the spatial and temporal variability of MPs in sediment from the Arctic Ocean. Furthermore, understanding is lacking on the correlation between Arctic sea ice variation and MP abundance in sediment. This study aimed to assess the MP contamination in the sediment from the Chukchi Sea over five years through three voyages (in 2016, 2018, and 2020). The MP abundances in the sediments from the Chukchi Plateau and Chukchi Shelf over five years ranged from 33.66 ± 15.08 to 104.54 ± 28.07 items kg^{-1} dry weight (DW) and 20.63 ± 6.71 to 55.64 ± 22.61 items kg^{-1} DW, respectively. The MP levels from the Chukchi Sea were lower than those from the Eastern Arctic Ocean. Our findings suggest that the Chukchi Plateau is an accumulation zone for fibers related to fishing gear and textiles under the dual influence of the Pacific and Atlantic Ocean currents. However, the reduction of these fibers in the sediment from the Chukchi Shelf might be related to bottom currents, sediment resuspension, and biomass. Moreover, the MP abundance in the sediment from the Chukchi Sea was positively correlated with the reduction of Arctic sea ice, suggesting that the melting sea ice contributes to the increase in MP levels in the sediment. The increase in blue MPs from the Chukchi Plateau over time might be attributed to melting sea ice or intense fishing activity, whereas the increase of the smallest MPs in this region could be owing to the breakdown of larger plastics during long-distance transport or the easier settlement of smaller MPs. Further time-series investigations are urgently required to improve the understanding of the environmental fate and transport of MPs among the different Arctic environmental compartments.

* Corresponding authors.
E-mail addresses: linlsh@tio.org.cn (L. Lin), bojun@tio.org.cn (J. Bo).

https://doi.org/10.1016/j.scitotenv.2021.150530
0048-9697/© 2021 Published by Elsevier B.V.

1. Introduction

Microplastics (MPs) are considered as globally ubiquitous emerging pollutants and have become a serious environmental concern in the Arctic because of their prevalence in various Arctic environmental compartments and their potential risks to polar wildlife (Bergmann et al., 2017a; Fang et al., 2018; Bergmann et al., 2019; Mu et al., 2019a; Kanhai et al., 2020; Tekman et al., 2020; Corsi et al., 2021). Increasing evidence shows that the Arctic Ocean is an accumulation area for MP particles, which could be mainly attributed to three reasons (Lima et al., 2021).

First, various local and distant sources exist that can contribute to the transport of MPs to Arctic regions. The local sources include increased shipping, tourism, fisheries, and resource exploitation owing to the continual decline in sea ice (Peeken et al., 2018b). Moreover, the “Big 6” and “Middle 8” rivers in the pan-Arctic watershed may deliver MPs from land-based sources into the Arctic Ocean (Holmes et al., 2013; Lebreton et al., 2017; Yakushev et al., 2021). The distant sources could lead to long-range transport of MPs by ocean currents and the atmosphere into the Arctic. There are two important ocean circulations in the Arctic Ocean, namely the Pacific and Atlantic Ocean currents, which can transfer floating debris from the subtropical ocean gyres to the Arctic Ocean (Cózar et al., 2017). The Pacific inflow originates from the North Pacific Ocean, crosses the Chukchi Sea, and then flows into the Atlantic Ocean via the Fram Strait and Canadian Archipelago by transpolar drift (Woodgate, 2013). The Atlantic inflow, which enters the Arctic Ocean through the Fram Strait and the Barents Sea flows along the slope of the Eurasian Basin, is saltier, warmer, and has a larger volume than the Pacific inflow (Woodgate, 2013). Subsequently, approximately half of this inflow moves north along the Mendeleev Ridge, a part of which continues to flow around the Chukchi Borderland and merges into the Beaufort Gyre (Woodgate, 2013; Dmitrenko et al., 2017; Forster et al., 2020). Onink et al. (2019) found that the Stokes drift contributes to MP transport from the North Pacific and North Atlantic Ocean gyres to the Arctic, emphasizing the importance of ocean transport processes in the global cycle of MPs.

Although limited information is available on the atmospheric transport of MPs in the Arctic, two recent studies found tiny MPs in the snow on the ice floes from the Fram Strait and Western Arctic Ocean (WAO), suggesting that snow function as a transport for airborne MPs to the Arctic (Bergmann et al., 2019; Kim et al., 2021). Recent studies have further proposed that atmospheric transport may play critical roles in delivering polyethylene terephthalate (PET) fibers and MPs from roads into the Arctic (Evangeliou et al., 2020; González-Pleiter et al., 2020). These findings confirm that the Arctic acts as a receiving region for MPs across the globe via atmospheric transport (Bergmann et al., 2019; Evangeliou et al., 2020).

Second, increasing evidence indicates that sea ice acts as an important temporary sink and vector for MPs, and can trap large quantities of MPs from the surrounding seawater and atmosphere (Peeken et al., 2018b; Tekman et al., 2020; Kim et al., 2021). These MPs may be released due to the melting of sea ice caused by continued warming of the Arctic atmosphere and ocean (Obbard et al., 2014; Bergmann et al., 2017b; Tekman et al., 2020). The most significant changes in sea ice occurred in the WAO, particularly in the Chukchi Sea, including the largest losses of summer sea ice in the Arctic Ocean and the continual decrease in the extent, coverage, and thickness of the sea ice (Stroeve and Notz, 2018; Kim et al., 2021). The WAO ice zone not only serves as a sink for global MPs, but also acts as a source of Arctic MPs (Kim et al., 2021). To date, limited information is available about the effects of sea ice on MP accumulation, which have mostly focused on the eastern Arctic, whereas data on the Chukchi Sea remain lacking (Bergmann et al., 2017b; Tekman et al., 2020; Kim et al., 2021). The Chukchi Sea can be divided into two regions in terms of plateau and shelf according to latitude and water depth (Lin et al., 2016; Marineregions.org, 2016). The environmental fate and behavior of MPs may differ between the Chukchi Shelf (CS) and Chukchi Plateau (CP) in consideration of the diverse geologic structures, ocean currents, and biodiversity (Woodgate, 2013; Lin et al., 2016; Mu et al., 2019a). However, the characteristics of MP pollution between these two regions have not yet been reported.

Third, Arctic sediment is considered as a potential sink for MPs in view of ubiquitous MPs in the sediments from Fram Strait, Svalbard, Barents, Norwegian Seas, Arctic Central Basin, eastern Canadian Arctic, northern Bering and Chukchi Seas (Bergmann et al., 2017b; Lots et al., 2017; Kanhai et al., 2019; Mu et al., 2019a; González-Pleiter et al., 2020; Huntington et al., 2020; Knutsen et al., 2020; Tekman et al., 2020). When sediment environmental conditions changed, the MPs in sediment would be released again and cause secondary pollution (Chen et al., 2021). The highly dynamic of the benthic environment of the Chukchi Sea due to intense cyclones, strong currents, and tides may make the sediment-bound MPs more likely to be re-suspended and redistributed (Zeng et al., 2017; Chen et al., 2021). However, knowledge of the long-term spatial and temporal variability of MPs in Arctic sediment, especial for the Chukchi Sea, remains limited (Bergmann et al., 2017b).

Overall, the aims of this study were to assess (i) the spatial and temporal variability of MPs in the sediment from the Chukchi Sea, (ii) the characteristics of MP pollution between the CS and the CP, (iii) potential sources and accumulation zones of sedimentary MPs in the Chukchi Sea, and (iv) possible interactions between Arctic sea ice variations and MP abundances in the sediment. Therefore, in this study, the MP contamination in the sediment from the Chukchi Sea over five years was investigated through three voyages (in 2016, 2018, and 2020) of the Chinese National Arctic Research Expedition.

2. Materials and methods

2.1. Field sampling

A total of 37 sampling stations in the CP and CS were investigated through the 7th, 9th, and 11th Chinese National Arctic Research Expedition (CHINARE-Arctic) in 2016, 2018, and 2020, respectively (Fig. 1a). For the division of the Chukchi Sea into CP and CS, the minimum latitude of CP was 74.78°N, and the water depth of CP was more than 200 m (Lin et al., 2016; Marineregions.org, 2016). Specifically, 21, 9, and 7 stations were sampled in 2016, 2018, and 2020, respectively. The annotation of each station located in different regions is presented in Fig. 1b and c. Although it was difficult to ensure that the sampling stations remained identical over the different years, four stations over the three voyages were the same, namely P11 and P3-7 in the CP and R12 and R1 in the CS (Fig. 1b and c). The detailed location coordinates for each station is shown in Table 1 of the Supplementary Material (Table S1).

The sediment samples were collected using a 50 cm × 50 cm × 65 cm stainless-steel box corer (200 kg) on a research icebreaker (R/V Xuelong). Approximately 500 g of surface sediment from the top up to 5 cm depth was carefully collected using a stainless-steel scoop (Mu et al., 2019a). Then, the sediments were wrapped with aluminum foil and kept in clean sealed bags, which were stored at -20 °C for further treatment.

2.2. Quality assurance/quality control (QA/QC)

QA/QC was performed as described in our previous studies (Fang et al., 2018; Mu et al., 2019a; Fang et al., 2021). In short, no plastic material was used during the entire experiment, and all reagents were filtered over a cellulose nitrate membrane filter (Whatman GF/A; 1.6 μm pore size with a 47 mm diameter). Both the samples and the non-plastic equipment were strictly protected to reduce the opportunity for exposure to plastics. Seven procedural blanks without sediments were performed simultaneously with the samples to monitor background contamination. Moreover, four clean cellulose nitrate membrane filters were placed around the microscope during microscopic examination to monitor airborne contamination.

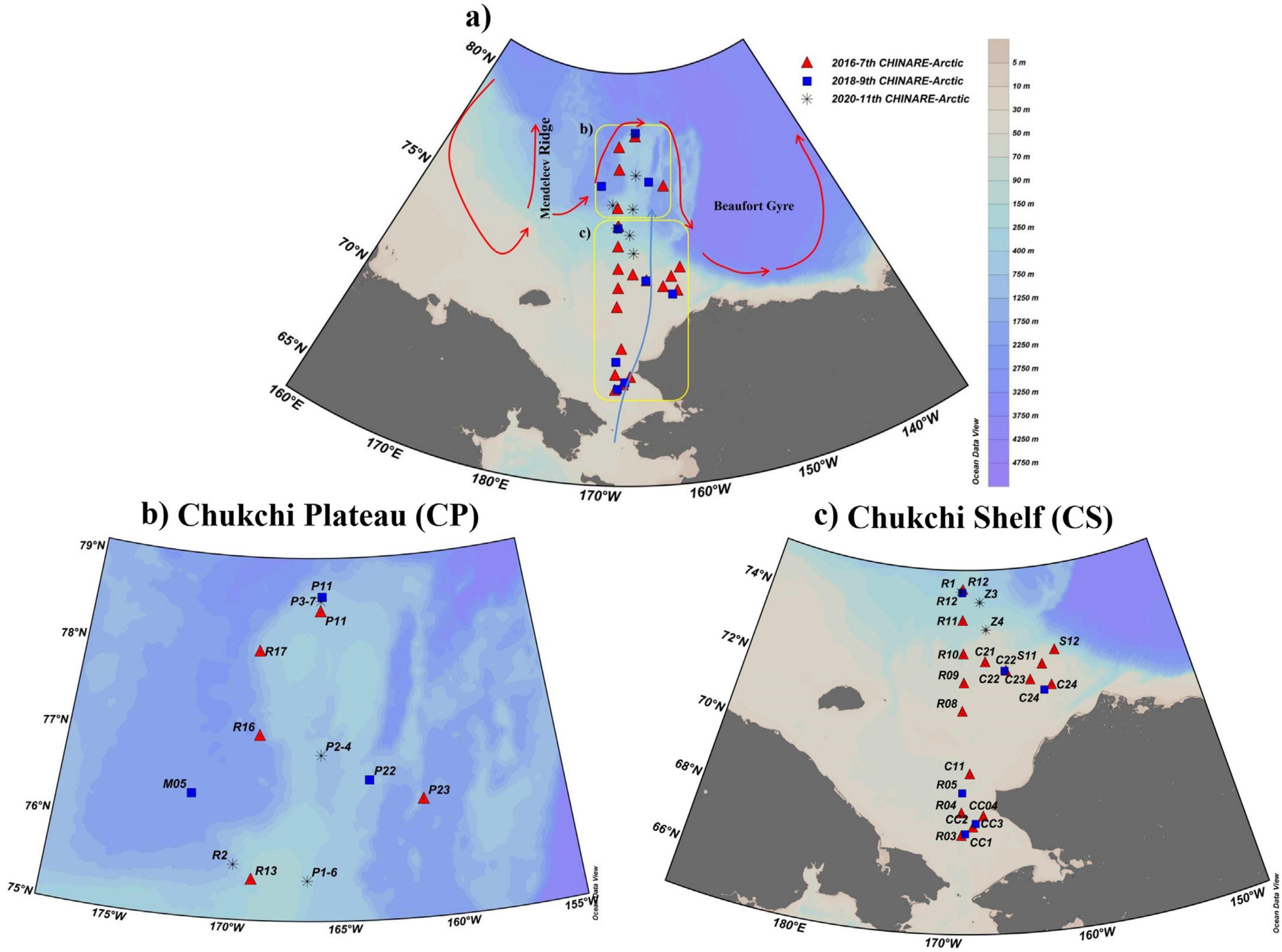

Fig. 1. (a) General overview of the sampling sites in the Chukchi Sea and (b, c) geographical location and annotation of each site in the Chukchi Plateau (CP) and Chukchi Shelf (CS). Schematic diagram of the circulation of the Atlantic Water (red arrows) and Pacific Water (light blue arrows), obtained by referring to previous studies (Dmitrenko et al., 2017; Forster et al., 2020; Woodgate, 2013).

2.3. Microplastic extraction and analysis

MP extraction from the sediment was conducted as previously described, with minor modifications (Mu et al., 2019a; González-Pleiter et al., 2020; Cincinelli et al., 2021). In short, the sediment samples were covered with aluminum foil and dried at 60 °C in an oven to a constant weight. Approximately 100 g dry weight (dw) sediment was placed in a 2 L glass beaker with the same volume of saturated NaCl solution for density separation. The mixture was stirred for 1 h using a stainless-steel stirrer and allowed to stand overnight to improve separation. Afterward, the overlying solution was collected and successively filtered over 500 μm and 38 μm stainless-steel meshes. All the suspected MPs retained on the mesh with a larger aperture were removed after visual observation and stored in a glass Petri dish for further analysis. Moreover, all the materials on the mesh with a smaller aperture were transferred to another glass beaker by rinsing with 10% KOH (W/V) solution. Then, the volume of KOH was adjusted to approximately three times that of the samples and placed in an oscillation incubator for 6 h at 60 °C and 300 rpm to remove organic matter. Subsequently, all the digestion solutions were filtered over GF/A filters (1.6 μm pore size and 47 mm diameter) under vacuum conditions. Finally, the filters were stored in glass Petri dishes for further analyses. The extraction process was repeated thrice.

The suspected MPs on the filters were collected and photographed using a Nikon P-RN2 stereo microscope with a DS-Fi3 charge-coupled device (CCD) camera (Nikon Corporation, Japan). A total of 499 suspected MPs were transferred to an alum-coated microscope slide (Thermo Fisher Scientific, USA) and identified using Fourier transform infrared microscopy in reflection mode (μ-FTIR, Nicolet iN10, Thermo Fisher Scientific Inc.). The samples' spectra were recorded in the spectral wavenumber range of 675 to 4000 cm^{-1} with co-scan 16 times at a resolution of 4 cm^{-1}. The resulting spectra were compared with the Bruker FTIR library, and the acceptable match ratio of successful identification was >70%.

2.4. Arctic sea ice index analysis

As the months of March and September represent the maximum and minimum extents of typical Arctic sea ice, respectively, this study focused on these two months' sea ice indices in the three voyages (Peeken et al., 2018a). The Arctic sea ice index data, which were extracted from the National Snow & Ice Data Center, comprised monthly sea ice extent, concentration, and anomalies (National Snow and Ice Data Center, 2021). The decrease rate constants of Arctic sea ice extent and concentration from March to September were calculated using the slope function in Excel. The sea ice anomalies were calculated as follows:

$$A = \frac{E - E'}{E'} \times 100\% \quad (1)$$

where A is the sea ice anomaly, E is the mean sea ice extent value for the studied month, and E′is the mean sea ice extent value for the studied month during 1981–2010 (National Snow and Ice Data Center, 2021).

2.5. Statistical analysis

The data for the MP abundance in the sediment was expressed as the mean ± standard error (S.E.). Statistical analysis was performed using SPSS (version 16.0; SPSS Inc., Chicago, Illinois, USA). First, the normality of the data was tested using the Shapiro-Wilk test. If the data showed a normal distribution, then a homogeneity test of variances was conducted using the Levene's test. When equal variance was confirmed, the independent sample *t*-test was used to examine the significant differences in MP abundances between different voyages. If the data showed an abnormal distribution or unequal variance, a non-parametric test followed by the Mann-Whitney *U* test was performed. The correlations between the MP abundances and sea ice indices were analyzed using bivariate correlations followed by Spearman correlation coefficients with a two-tailed test. Differences were considered significant at $p < 0.05$.

3. Results

3.1. Background contamination of MPs

Various fibers were observed in the procedural blanks and filters. The abundances of blue, black, and red fibers with the composition of rayon were 0.18, 0.09, and 0.09 items/filter, respectively. The abundances of blue fiber with the composition of polyacrylamide (PAM), the black fibers with the compositions of PET and leather, and the transparent fiber with the composition of polyester (PES) were all 0.09 items/filter. These detected values of the fibers were subtracted from the final results of this study.

3.2. Spatio-temporal variation of MP contamination in the sediment

Fibers constituted the predominant shape (80%–92%) of MPs in the sediment, followed by fragments (4%–16%) and films (3%–4%) over the three voyages. Representative photographs of MPs with different types are shown in Fig. 1 of the Supplementary Material (Fig. S1). The total MP abundance in the CP sediment in 2020 was 210.55% and 132.61% higher than that in 2016 ($p = 0.07$) and 2018, respectively (Fig. 2). In contrast, the total MP abundance in the CS sediment in

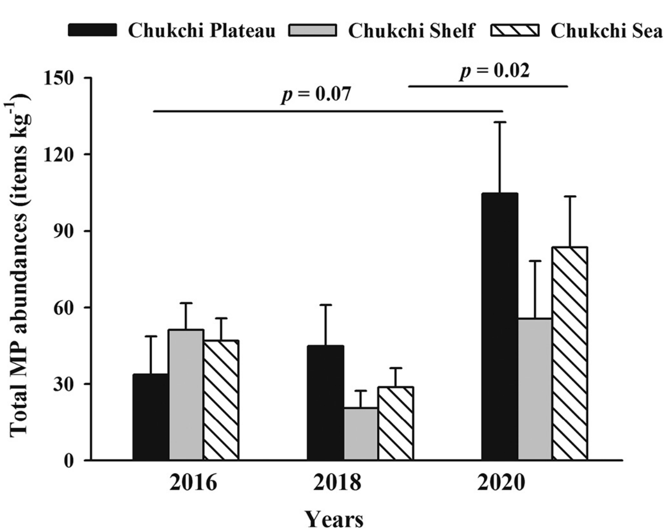

Fig. 2. Total MP abundances in the sediments from the CP, CS and Chukchi Sea over five years determined through the three voyages (in 2016, 2018, and 2020). Differences were considered significant at $p < 0.05$.

2016 was comparable with that in 2018 and 2020 (Fig. 2). Overall, the total MP abundance in the Chukchi Sea sediment in 2020 was significantly higher ($p = 0.02$) than that in 2018 (Fig. 2). The total MP abundances in 2016 and 2018 considered as a whole was also significantly lower ($p = 0.04$) than that in 2020. The detailed total MP abundance data for each station is shown in Table S1.

3.3. Spatio-temporal variation of MP compositions in the sediment

In this study, 155 suspected MPs (31%) were eventually identified as MPs and the compositions of MPs were divided into three categories based on their applications. The infrared spectra of all representative MP compositions and their corresponding reference spectra are shown in Fig. S2.

Synthetic fibers composed of polyamide (PA), PES, polyethylene (PE), polypropylene (PP), polyvinyl alcohol (PVA), and polyvinyl chloride (PVC) are commonly used in fishing gear materials (Thomas and Manju Lekshmi, 2017). The variations in the percentage and abundance of these fibers in the sediment across the CP and CS sites showed opposite trends. For example, these fibers detected in the CP sediment in 2020 were 158.60% and 64.15% higher in percentage than those in 2016 and 2018, respectively (Fig. 3a). In contrast, these fibers in the CS sediment in 2020 were 19.97% and 37.07% lower in percentage than those in 2016 and 2018, respectively (Fig. 3a). Moreover, these fibers in the CP sediment in 2020 were 336.58% and 134.69% higher in quantity than those in 2016 ($p = 0.08$) and 2018, respectively (Fig. 3b). However, these fibers detected in the CS sediment in 2020 were 72.14% and 55.96% less in quantity than those in 2016 and 2018, respectively (Fig. 3b). Overall, these fibers related to fishing gear materials in the Chukchi Sea sediment in 2020 were 36.19% and 6.49% higher in percentage than those in 2016 and 2018, respectively (Fig. 3a). The corresponding abundances of these fibers in 2020 were 70.93% and 99.22% higher than those in 2016 and 2018, respectively (Fig. 3b).

Synthetic fibers consisting of acrylic, PES, PET, rayon, and yarn are widely used in textiles. Higher variations in the percentage and abundance of these fibers were observed in the sediment from the CP than those from the CS. For example, these fibers in the CP sediment in 2020 were 22.48% and 52.21% higher in percentage than those in 2016 and 2018, respectively (Fig. 4a). In contrast, these fibers in the CS sediment in 2020 were 15.94% and 45.68% higher in percentage than those in 2016 and 2018, respectively (Fig. 4a). Moreover, these fibers in the CP sediment in 2020 were 196.99% and 284.97% higher in quantity than those in 2016 ($p = 0.07$) and 2018 ($p = 0.09$), respectively (Fig. 4b). Contrarily, these fibers in the CS sediment in 2020 were 3.53% less and 195.58% higher in quantity than those in 2016 and 2018, respectively (Fig. 4b).

Overall, the fibers related to the textiles in the Chukchi Sea sediment in 2020 were 31.19% and 59.12% higher in percentage than those in 2016 and 2018, respectively (Fig. 4a). The corresponding abundances of these fibers in 2020 were 78.45% and 310.74% higher than those in 2016 ($p = 0.09$) and 2018 ($p = 0.01$), respectively (Fig. 4b).

MPs composed of PAM, polybutadiene (PB), polycarbonate (PC), polyphenylene sulfide (PPS), rubber, and resin are mainly applied in engineering and industry. The compositions of these MPs in the sediment from the CP and CS varied significantly for different voyages. The percentage and abundance of PAM increased in the CS sediment from 2016 to 2018 (Fig. 5a and b). Although PAM from the CS was not detected thereafter, it was present in the CP sediment in 2020 (Fig. 5a and b).

The percentage and abundance of rubber first decreased and then increased in the CS sediment from 2016 to 2020 (Fig. 5a and b). In contrast, the percentage and abundance of rubber first increased and then decreased in the CP sediment from 2016 to 2020 (Fig. 5a and b). In particular, rubber was found at the near-shore station (CC04) and the R1 station adjacent to the Chukchi Borderland in 2016 and 2020. Resin was detected both in the CS and CP sediments in 2016 and 2020

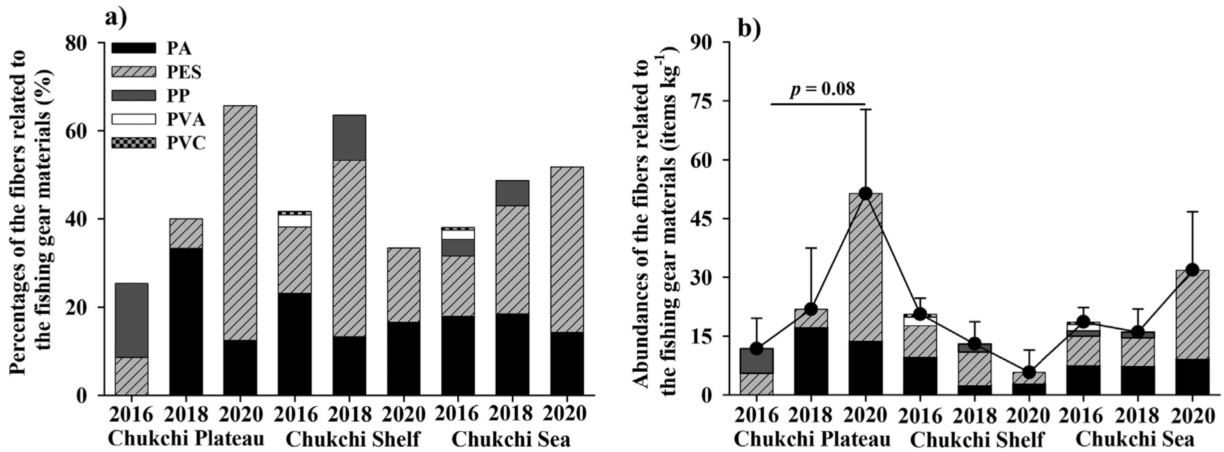

Fig. 3. (a) Percentages and (b) abundances of the fibers related to the fishing gear materials in the sediments from the CP, CS, and Chukchi Sea over five years determined through the three voyages. PA: polyamide; PES: polyester; PP: polypropylene; PVA: polyvinyl alcohol; and PVC: polyvinyl chloride. Differences were considered significant at $p < 0.05$.

(Fig. 5). Furthermore, PB, PC and PPS were only found in the sediment from either the CP or CS in 2016 or 2018 (Fig. 5).

3.4. MP contamination in the sediments at the same stations

Similar changing trends of MPs in the sediment were also observed at the same stations from the CP (P11 and P3-7) and CS (R12 and R1) over the three voyages. For example, the amounts of fibers related to fishing gear and textiles in the sediment at P3-7 in 2020 were higher than those at P11 in 2016 and 2018 (Table S2). In contrast, the amounts of these fibers in the sediment at R1 in 2020 were lower than those at R12 in 2016 or 2018 (Table S2). Furthermore, the MP levels related to engineering and industry were only detected in the sediment at R1 in 2020 (Table S2).

3.5. Spatio-temporal variation of MPs with different colors in the sediment

In the CP sediment, black MPs accounted for the largest proportion of the total MPs, followed by blue and transparent MPs in 2016 and 2020, respectively (Fig. 6a). The gray MPs constituted the largest percentage of the total MPs from the CP in 2018 followed by blue and transparent MPs. In the CS sediment, the black MPs accounted for the largest proportion of the total MPs over the three voyages (Fig. 6a). Overall, the black MPs accounted for the largest proportion of the total MPs from the Chukchi Sea over the three voyages (Fig. 6a). The blue and transparent MPs accounted for the second largest proportion of the total MPs from the Chukchi Sea in 2016 and 2020, whereas the gray and blue MPs accounted for the second largest proportion of the total MPs from the Chukchi Sea in 2018. Representative photographs of MPs with different colors are shown in Fig. S1.

In particular, the blue MPs in the CP sediment in 2020 were 114.81% and 46.46% higher in percentage than those in 2016 and 2018, respectively (Fig. 6a). The blue MPs in the CP sediment in 2020 were 303.88% and 88.64% higher in quantity than those in 2016 ($p = 0.09$) and 2018, respectively (Fig. 6b). Overall, the blue MPs in the sediment from the Chukchi Sea in 2020 were 48.00% and 43.31% higher in percentage than those in 2016 and 2018, respectively (Fig. 6a). Accordingly, the blue MPs in the Chukchi Sea sediment in 2020 were 124.88% and 220.56% higher in quantity than those in 2016 and 2018, respectively (Fig. 6b).

3.6. Spatial and temporal variations in sizes of the MPs in the sediment

The sizes of the MPs in the sediment from the Chukchi Sea in 2016 ranged from 0.23 mm to 4.23 mm, with an average size of 1.48 mm in the CP and 1.37 mm in the CS; those in 2018 ranged from 0.25 mm to 3.27 mm, with an average size of 1.15 mm in the CP and 1.68 mm in the CS; and those in 2020 ranged from 0.19 mm to 5.00 mm, with an average size of 1.29 mm in the CP and 1.31 mm in the CS.

All sizes of MPs considered in this study were divided into eight groups: 0.19–0.50 mm, 0.50–1.00 mm, 1.00 mm–1.50 mm, 1.50 mm–2.00 mm, 2.00 mm–2.50 mm, 2.50 mm–3.00 mm, 3.00 mm–3.50 mm,

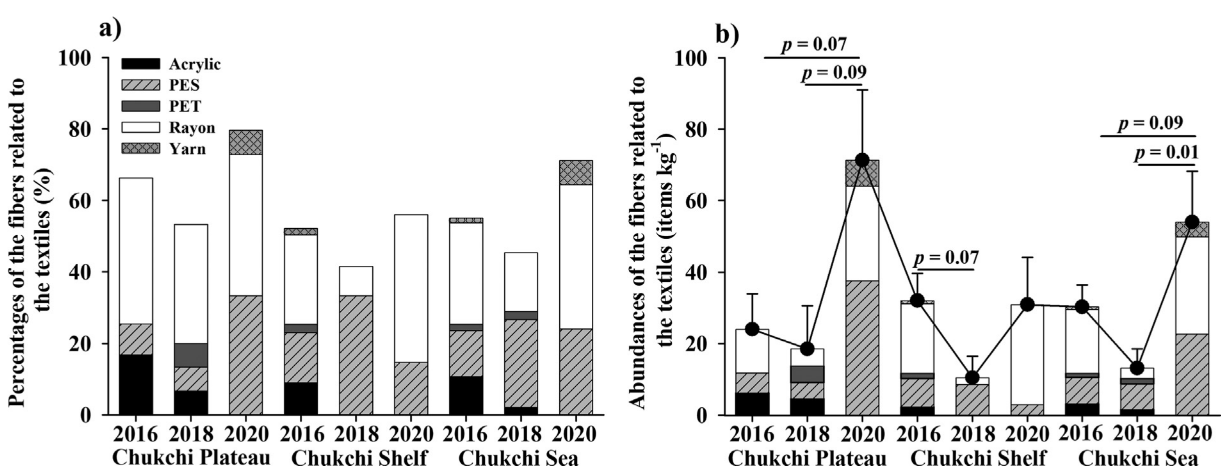

Fig. 4. (a) Percentages and (b) abundances of the fibers related to the textiles in the sediments from the CP, CS, and Chukchi Sea over five years determined through the three voyages. PET: polyethylene terephthalate. Differences were considered significant at $p < 0.05$.

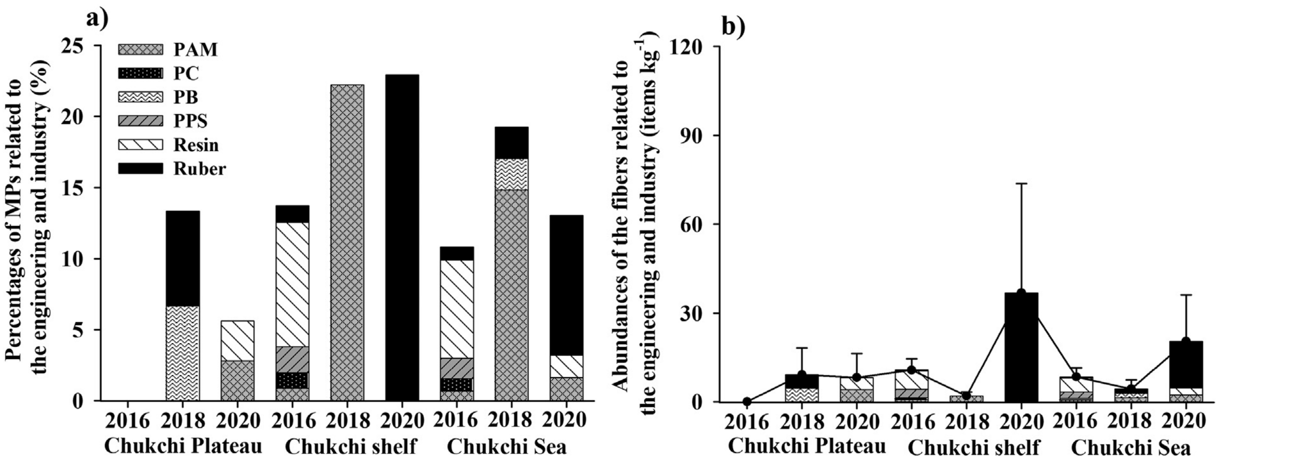

Fig. 5. (a) Percentages and (b) abundances of the MPs related to the engineering and industry in the sediments from the CP, CS, and Chukchi Sea over five years determined through the three voyages. PAM: polyacrylamide; PB: polybutadiene; PC: polycarbonate; and PPS: polyphenylene sulfide.

and 3.50 mm–5.00 mm. The MPs ranging 0.19–0.50 mm in the CP sediment were not detected in 2016 and these MPs in 2020 were 278.39% higher in percentage than those in 2018 (Fig. 7a). Accordingly, the abundances of MPs for the same size range in the CP sediment in 2020 were significantly higher ($p = 0.03$) than that in 2016 (Fig. 7b). Overall, the MPs ranging 0.19–0.50 mm in the Chukchi Sea sediment in 2020 were 107.69% and 108.93% higher in percentage than those in 2016 and 2018, respectively (Fig. 7a). The corresponding abundances of MPs for the same size range in the Chukchi Sea sediment in 2020 were significantly higher than those in 2016 ($p = 0.01$) and 2018 ($p = 0.04$) (Fig. 7b).

3.7. Correlations between the MP abundances and Arctic sea ice indices

The Arctic sea ice extent and concentration gradually decreased from March to September over the three voyages (Table S3). The decrease rate constant of Arctic sea ice extent and concentration for this period, along with the Arctic sea ice anomalies in September, were significantly positively correlated (R = 1.00, $p = 0.00$) with the abundances of fibers related to the textiles in the CP sediment and with the abundances of MPs related to engineering and industry application, as well as the total MP abundance in the CS sediment (Table S4). Overall, the significantly positive correlations (R = 1.00, $p = 0.00$) between the Arctic sea ice indices and MP abundances were all observed in the sediment from the Chukchi Sea (Table S4).

4. Discussion

In this study, we found that compared to 2016 and 2018, the MP abundance in the sediment in 2020 increased by 0.78- to 1.91-fold in the Chukchi Sea and 1.33- to 2.11-fold in the CP, respectively. This trend is consistent with those reported in previous studies in other sea areas. For example, MP abundance has increased by two orders of magnitude over the past four decades (1972–2010) in the North Pacific Subtropical Gyre (Goldstein et al., 2012). The concentration of MPs is estimated to increase four-fold by 2060 at approximately 30°N in the Pacific Ocean, whereas it may double by 2050 or increase 50-fold between 2010 and 2100 in the global ocean (Isobe et al., 2019; Lebreton et al., 2019). The average MP abundance in the sediment of the Chukchi Seas from 2016 to 2020 was higher than that in 2017, indicating the increase of MP levels over time (Mu et al., 2019a). However, the levels of MPs in the CP and CS sediments were obviously lower than those reported in the Eastern Canadian Arctic, Arctic Central Basin, Fram Strait, North Sea, and Barents Sea (Table 1), which is partially explained by the different analytical methods and the higher MP abundance in the Eastern Arctic Ocean than in the WAO (Ross et al., 2021).

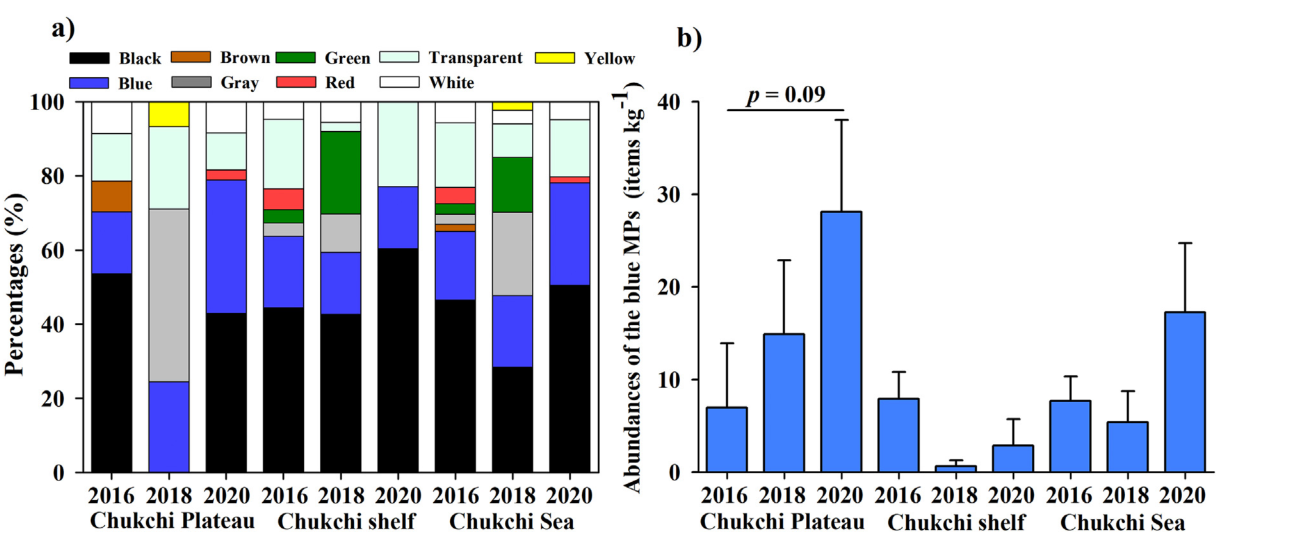

Fig. 6. (a) Percentages of the MPs with different colors and (b) abundances of the blue MPs in the sediments from the CP, CS, and Chukchi Sea over five years determined through the three voyages. Differences were considered significant at $p < 0.05$.

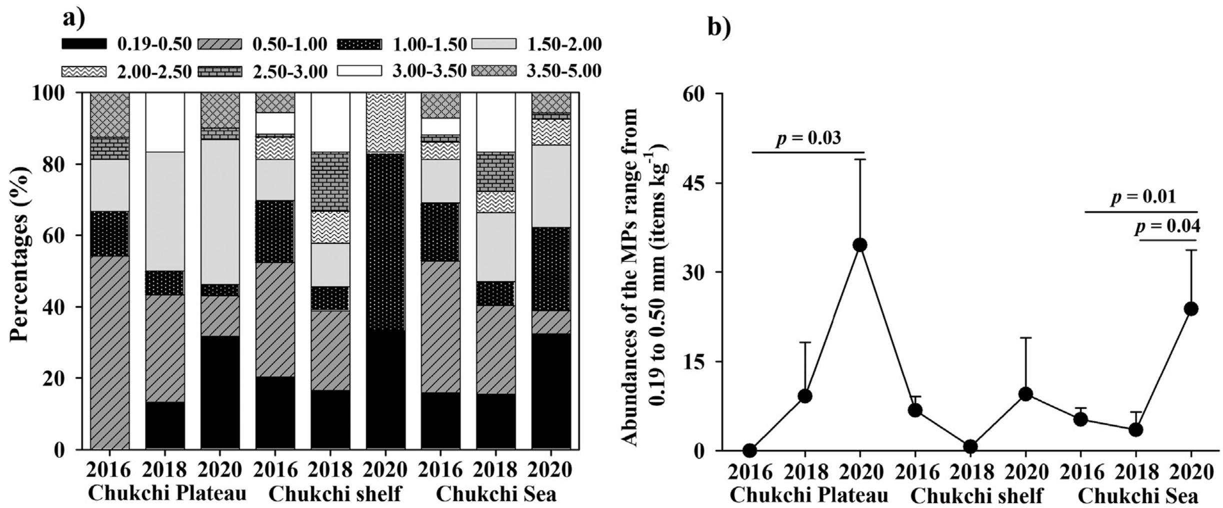

Fig. 7. (a) Percentages of the MPs with different sizes and (b) abundances of the MPs ranging 0.19–0.50 mm in the sediments from the CP, CS, and Chukchi Sea over five years determined through the three voyages. Differences were considered significant at $p < 0.05$.

PES and PA were the dominant components related to fishing gear materials, while rayon and PES were the major components related to textiles. Previous studies have found PES and PA to be the major components of MPs in the sea ice core, surface and sub-surface waters, benthic organisms, and snow from the Chukchi Sea, Arctic Central Basin, and Fram Strait, suggesting interactions between MPs and multimedia in the Arctic (Kanhai et al., 2018; Bergmann et al., 2019; Mu et al., 2019b; Kanhai et al., 2020; Kim et al., 2021). Rayon, a semi-synthetic fiber, is widely used in textiles and personal hygiene products (J. Zhao et al., 2018; Mu et al., 2019a; Zhang et al., 2019). It has also been reported as one of the most common polymers in the surface sediments of the Bering Sea-Chukchi Sea Shelf (Mu et al., 2019a). Moreover, rayon has been widely detected in deep-sea sediments from sub-Arctic regions in the North Atlantic Ocean and Arctic sea ice (Obbard et al., 2014; Woodall et al., 2014).

The views of the region and the same stations revealed that the increase in fibers related to fishing gear materials and textiles in the CP was more significant than that in the CS. These findings might be attributed to Arctic sea ice variations, ocean currents, atmospheric transport, and biomass. Although the deposition pathways of MPs from the ocean surface to the sediment remain largely unknown, biofouling, marine aggregates, and density settlement act as potential contributing factors (Galloway et al., 2017; S. Zhao et al., 2018). In addition, near-bed thermohaline currents (bottom currents) can control the distribution and accumulation of sediments along with the MPs on the seafloor (Kane et al., 2020). Furthermore, the benthic environment of the Chukchi Sea is highly dynamic, which could promote sediment resuspension, accompanied by the release of sediment-bound MPs (Zhang et al., 2013; Zeng et al., 2017; Chen et al., 2021).

The HAUSGARTEN observatory in the Fram Strait found that the Arctic deep-sea sediment at the northernmost stations, which are located within or close to the long-lasting marginal ice zone, accumulated the highest quantities of MPs compared to the stations at lower latitudes (Bergmann et al., 2017b). Over 1 trillion pieces of plastic were estimated to have been released from the Arctic sea ice because the thickness and extent of the sea ice have shown a declining trend (Obbard et al., 2014). Moreover, the CP is nearer to the marginal ice zone than the CS, particularly in September (National Snow and Ice Data Center, 2021). Peeken et al. (2018b) showed that sea ice originating from the Makarov Basin, which is also located closer to the CP than the CS, accumulated considerable levels of MPs. Furthermore, the most notable decreases in Arctic sea ice indices occurred in 2020, and a significant positive correlation was found between the receding sea ice and the abundances of textile fibers, suggesting that the melting Arctic sea ice may play an important role in driving the increase of the textile fibers in the CP sediment.

The patterns of ocean currents indicate that the CP is like a crossroad between the Pacific and Atlantic Ocean currents. The North Pacific seawater contains higher MP levels than other global seawater because of the North Pacific garbage patch (Van Sebille et al., 2015; Isobe et al., 2019). Additionally, higher fishing intensity and concentration of main ports in the Arctic and sub-Arctic are observed around the Barents, Norwegian, North, and Bering Seas as well as the Northeast Atlantic Ocean and Gulf of Alaska (PAME, 2019). Furthermore, Ross et al. (2021) reported that Atlantic current can deliver a high quantity of textile fibers into the Arctic Ocean. Consequently, the CP could probably be regarded as an accumulation zone of MPs, particularly for the fibers related to fishing gear materials and textiles, under the dual influence of the Pacific and Atlantic inflows.

However, the depth of seawater at the stations in the CP, which is composed of Atlantic Water and Arctic Deep Water, ranged from 222 m to 2293 m (Aagaard and Carmack, 1989). The Atlantic Water is a major contributor to the widespread distribution of PES fibers in the Arctic Ocean owing to textiles, laundry, and wastewater discharges (Ross et al., 2021). The Arctic Deep Water receives the inflows from Greenland and Norwegian Sea deep water, which also originate from the hotspot of MP pollution (Lusher et al., 2015; Bråte et al., 2018; Morgana et al., 2018; Jiang et al., 2020). Therefore, the Atlantic Water and Arctic Deep Water may make a significant contribution to increasing MPs in the sediment of the CP.

In contrast, our data showed that the MP abundances related to fishing gear and textile fibers, were decreased in the sediment of CS in 2018 and 2020. These findings may be attributed to the resuspension of these MPs due to the Arctic cyclone, and MPs could be transported from the CS to the CP through the Pacific inflow (Woodgate, 2013; Zeng et al., 2017; Day et al., 2018; Chen et al., 2021). Additionally, the bottom currents might also play a crucial role in transferring these MPs on the Arctic seafloor. Our previous study indicated that sea anemones inhabiting the CS ingested higher quantities of MPs than those inhabiting the CP in 2018 (Kane et al., 2020; Fang et al., 2021). Therefore, higher quantities of benthos in the CS may lead to absorption of higher amounts of MPs from the sediment, which could also affect the distribution patterns of sediment-bound MPs.

Field-based evidence has shown that atmospheric transport and deposition is another notable pathway for transport of terrestrial MPs to the ocean, particularly for textile microfibers such as, PET, PAN, and rayon (Liu et al., 2019). Global distillation and cold condensation effects

Table 1
Microplastic abundances reported in the sediments around the Arctic Ocean.

Study	Location	Depth	Sampling Equipment	Microplastic abundances	Microplastic compositions
Shore line					
Dippo (2012)	Western Iceland	Top 2 cm of the beach sediment	Shallow metal scoop	ND[b]–34 items L^{-1} sediment	NA
Whitmire and Van Bloem (2017)	Six national park beaches located in the Western Arctic and the Gulf of Alaska	Top 1.5 cm of the beach sediment	Metal ring and metal spoon	40–129 items kg^{-1} dry weight	NA
Lots et al. (2017)	Vik, Iceland	Top 5 cm of the beach sediment	Metal spoon	792 ± 128 items kg^{-1} dry weight	PES, PE, PP
Lots et al. (2017)	Tromsø, Smøla and Drøbak, Norway	Top 5 cm of the beach sediment	Metal spoon	72–100 items kg^{-1} dry weight	PES, PE, PP
Lots et al. (2017)	Kalundburg, Fyns Hoved and Bjerge Nord, Denmark	Top 5 cm of the beach sediment	Metal spoon	88–164 items kg^{-1} dry weight	PES, PE, PP
Sundet et al. (2016)	Svalbard, Adventdalen	Beach sediment	Shovel	ND–6.4 items kg^{-1} dry weight	NA
Sundet et al. (2017)	Svalbard, Breibogen	Beach sediment	Shovel	5–111 items L^{-1} sediment	NA
Shallow water					
Sundet et al. (2016)	Svalbard, Adventfjorden	40–70 m	Van Veen grab	ND–9.2 items kg^{-1} dry weight	NA
Sundet et al. (2017)	Svalbard, Breibogen	40–60 m	Van Veen grab	2–10 items L^{-1} sediment	NA
Lilleeng (2018) and Møskeland et al. (2018)	The central North Sea	66–80 m	Van Veen Grab samplers	412 ± 770 to 6155 ± 7003 items kg^{-1} dry weight	PAM and phenoxy resin
Mu et al. (2019a)	Bering and Chukchi Seas	35–178 m	Box corer	ND–68.78 items kg^{-1} dry weight	PP, PET
González-Pleiter et al. (2020)	Freshwater Arctic lake, Svalbard Archipelago	≦0.75 m	NA	400 items m^{-2}	PET
Huntington et al. (2020)	Eastern Canadian Arctic	NA [a]	Box corer	1940 items kg^{-1} dry weight	PET
This study (2016-2020)	Chukchi Shelf	36–318 m	Box corer	20.63 ± 6.71 to 55.64 ± 22.61 items kg^{-1} dry weight	PES, PA, Rayon
Deep sea					
Bergmann et al. (2017b)	HAUSGARTEN observatory, Fram Strait	2340–5570 m	Multiple corer	42–6595 items kg^{-1} dry weight	PE, PA, PP
Lilleeng (2018) and Møskeland et al. (2018)	The northern North Sea	137–400 m	Van Veen Grab samplers	677 ± 1064 to 2333 ± 2920 items kg^{-1} dry weight	PE-chlorinated, rubber and "other" plastics
Lilleeng (2018) and Møskeland et al. (2018)	The Barents Sea	251–508 m	Van Veen Grab samplers	452 ± 385 to 1570 ± 1157 items kg^{-1} dry weight	PE-chlorinated, PE:PP, rubber and paint
Kanhai et al. (2019)	Arctic Central Basin (11 sites)	855–4353 m	Gravity corer or piston corer	ND–220 items kg^{-1} dry weight	PES, PS, PA, PAN, PP, PVC
Tekman et al. (2020)	HAUSGARTEN observatory, Fram Strait	2449-5350 m	Multiple corer	239–13,331 items kg^{-1} dry weight	PE
Woodall et al. (2014)	Southwest of Svalbard	1000 m	Megacorer/boxcorer	200 items L^{-1} sediment	PES, Rayon
Woodall et al. (2014)	Southwest of Svalbard	2000 m	Megacorer/boxcorer	300 items L^{-1} sediment	Acrylic, PES, Rayon
This study (2016-2020)	Chukchi Plateau	222–2293 m	Box corer	33.66 ± 15.08 to 104.54 ± 28.07 items kg^{-1} dry weight	PES, PA, Rayon

PA: polyamide (Nylon); PAM: polyacrylamide; PAN: polyacrylonitrile; PE: polyethylene; PES: polyester; PET: polyethylene terephthalate; PP: polypropylene; PS: polystyrene; PVC: polyvinyl chloride.
[a] NA means no data.
[b] ND means not detected.

are known to enhance the atmospheric deposition of persistent organic pollutants at high latitudes with low temperatures, which may also be one of the factors leading to higher fiber accumulation in the CP than in the CS (Blais et al., 1998; Scheringer et al., 2000).

Considering the changing trends of MP abundance related to engineering and industry, the presence of PAM, resin, and rubber in the CP and CS might be interlinked. PAM is an engineering plastic that is commonly used in various industrial applications, such as oil and gas extraction (Xiong et al., 2018). Resin is used as an additive in oil-well cementing to ensure the drilling and completion of oil or gas wells (Al-yami et al., 2017). Rubber is present in snow from ice floes, sea ice, and deep-sea sediments in the Arctic, indicating that this polymer could be transported to sea ice and the seafloor through the atmosphere (Bergmann et al., 2017b; Peeken et al., 2018b; Bergmann et al., 2019). From the variation patterns of these MPs, the PAM and resin may be considered to have originated from the CS owing to offshore oil and gas exploration, and transported to the CP via transpolar drift (Wilson et al., 2018; Halsband and Herzke, 2019). Furthermore, rubber may be transported from the near-shore station in the CS to site R1 via the transpolar drift or from the CP to site R1 via the Atlantic current. The temporal trends of other related MPs varied widely, suggesting that their emission sources may be unstable and require continuous monitoring.

Our results revealed a prevalence of MPs with black, blue, transparent and gray colors in the sediment from the Chukchi Sea. The black and blue colors were also the most common colors in seawater, sediment, and sea ice from other Arctic regions, Arctic adjacent oceans, and European beach (Lusher et al., 2014; Obbard et al., 2014; Woodall et al., 2014; Lusher et al., 2015; Lots et al., 2017; Mu et al., 2019b; Kanhai et al., 2020; von Friesen et al., 2020). Likewise, the gray MPs were also detected in the seawater, sediment and sea ice cores from Northeast Atlantic Ocean, European beach, Northeast Greenland and Arctic Central Basin (Lusher et al., 2014; Lots et al., 2017; Morgana et al., 2018; Kanhai et al., 2020). The transparent MPs were also detected in the seawater and sea ice cores from Arctic Central Basin (Kanhai et al., 2018; Kanhai et al., 2020). In particular, the increasing concentrations of blue MPs in the CP may be attributed to the melting sea ice as the Arctic sea ice accumulates a large proportion of blue MPs (Obbard et al., 2014; von Friesen et al., 2020). Moreover, the increase in blue fibers is also possibly related to the rapid increase in fishing activities in the Arctic because these fibers are widely used in fishing gear materials (Ferreira et al., 2018).

The continuous increase in the proportion of the smallest MPs in the CP may be owing to breakdown of larger plastics during long-distance transport (Ross et al., 2021). Furthermore, smaller MPs were found to sink more readily and faster than larger ones because of their larger specific surface area, which can promote the formation and increase the density of marine snow (Bergmann et al., 2017b; S. Zhao et al., 2018). Accordingly, smaller MPs are more likely to sink to deeper water in the CP than larger ones.

5. Conclusions

The time-series data in this study provide useful information for understanding the spatial and temporal variability of MPs in sediment of the Chukchi Sea. The overall results revealed an increasing tendency of MP abundance in the sediment from the Chukchi Sea, particularly the CP, in 2020 than in 2016 and 2018. The CP is probably an accumulation zone for the MPs, particularly the fibers related to fishing gear materials and textiles, under the dual influence of the Pacific and Atlantic inflows. Some MPs related to engineering and industrial applications might originate from local sources around the CS. Moreover, melting sea ice or intense fishing activity in the Arctic could contribute to an increase in blue MPs in the CP. The increase in the smallest MPs in the CP could be owing to breakdown of the larger plastics during long-distance transport or because the smaller MPs can sink deeper more easily. However, further study is required to improve the understanding of the sources and ecological implications of MPs in the Arctic sediment.

CRediT authorship contribution statement

Chao Fang: Conceptualization, Validation, Visualization, Formal analysis, Writing – original draft, Writing – review & editing. **Yusheng Zhang:** Investigation, Methodology. **Ronghui Zheng:** Methodology. **Fukun Hong:** Investigation. **Min Zhang:** Investigation. **Ran Zhang:** Investigation, Resources. **Jianfeng Mou:** Investigation, Resources. **Jingli Mu:** Visualization. **Longshan Lin:** Conceptualization, Project administration, Resources, Writing – review & editing. **Jun Bo:** Conceptualization, Supervision, Project administration, Writing – review & editing.

Declaration of competing interest

The authors declare that they have no known competing financial interests or personal relationships that could have appeared to influence the work reported in this paper.

Acknowledgments

This work was sponsored by the first batch of the Youth Innovation Fund Project of Xiamen in 2020 (3502Z20206099), the Chinese Arctic and Antarctic Administration, the National Key Research and Development Program of China (Grant No. 2019YFD0901101), and the National Natural Science Foundation of China (Grant Nos. 41977211, 42176171 and 41806135).

Appendix A. Supplementary data

Supplementary data to this article can be found online at https://doi.org/10.1016/j.scitotenv.2021.150530.

References

Aagaard, K., Carmack, E.C., 1989. The role of sea ice and other fresh water in the Arctic circulation. J. Geophys. Res.-Oceans 94, 14485–14498.

Al-yami, A.S., Ramasamy, J., Wagle, V., 2017. Chemical additives for oil well cementing. Res. Rev. J. Chem. 6, 1–14.

Bergmann, M., Lutz, B., Tekman, M.B., Gutow, L., 2017a. Citizen scientists reveal: marine litter pollutes Arctic beaches and affects wild life. Mar. Pollut. Bull. 125, 535–540.

Bergmann, M., Mützel, S., Primpke, S., Tekman, M.B., Trachsel, J., Gerdts, G., 2019. White and wonderful? Microplastics prevail in snow from the Alps to the Arctic. Sci. Adv. 5, eaax1157.

Bergmann, M., Wirzberger, V., Krumpen, T., Lorenz, C., Primpke, S., Tekman, M.B., Gerdts, G., 2017b. High quantities of microplastic in Arctic deep-sea sediments from the HAUSGARTEN observatory. Environ. Sci. Technol. 51, 11000–11010.

Blais, J.M., Schindler, D.W., Muir, D.C.G., Kimpe, L.E., Donald, D.B., Rosenberg, B., 1998. Accumulation of persistent organochlorine compounds in mountains of western Canada. Nature 395, 585–588.

Bråte, I.L.N., Hurley, R., Iversen, K., Beyer, J., Thomas, K.V., Steindal, C.C., Green, N.W., Olsen, M., Lusher, A., 2018. Mytilus spp. as sentinels for monitoring microplastic pollution in Norwegian coastal waters: a qualitative and quantitative study. Environ. Pollut. 243, 383–393.

Chen, L., Li, J., Tang, Y., Wang, S., Lu, X., Cheng, Z., Zhang, X., Wu, P., Chang, X., Xia, Y., 2021. Typhoon-induced turbulence redistributed microplastics in coastal areas and reformed plastisphere community. Water Res. 204, 117580.

Cincinelli, A., Scopetani, C., Chelazzi, D., Martellini, T., Pogojeva, M., Slobodnik, J., 2021. Microplastics in the Black Sea sediments. Sci. Total Environ. 760, 143898.

Corsi, I., Bergami, E., Caruso, G., 2021. Special issue plastics in polar regions. Environ. Int. 149, 106203.

Cózar, A., Martí, E., Duarte, C.M., García-de-Lomas, J., van Sebille, E., Ballatore, T.J., Eguíluz, V.M., González-Gordillo, J.I., Pedrotti, M.L., Echevarría, F., Troublè, R., Irigoien, X., 2017. The Arctic Ocean as a dead end for floating plastics in the North Atlantic branch of the thermohaline circulation. Sci. Adv. 3, e1600582.

Day, J.J., Holland, M.M., Hodges, K.I., 2018. Seasonal differences in the response of Arctic cyclones to climate change in CESM1. Clim. Dyn. 50, 3885–3903.

Dippo, B., 2012. Microplastics in the Coastal Environment of West Iceland. University Centre of the Westfjord, Iceland.

Dmitrenko, I.A., Kirillov, S.A., Rudels, B., Babb, D.G., Pedersen, L.T., Rysgaard, S., Kristoffersen, Y., Barber, D.G., 2017. Arctic Ocean outflow and glacier–ocean interactions modify water over the Wandel Sea shelf (northeastern Greenland). Ocean Sci. 13, 1045–1060.

Evangeliou, N., Grythe, H., Klimont, Z., Heyes, C., Eckhardt, S., Lopez-Aparicio, S., Stohl, A., 2020. Atmospheric transport is a major pathway of microplastics to remote regions. Nat. Commun. 11, 3381.

Fang, C., Zheng, R., Hong, F., Jiang, Y., Chen, J., Lin, H., Lin, L., Lei, R., Bailey, C., Bo, J., 2021. Microplastics in three typical benthic species from the Arctic: occurrence, characteristics, sources, and environmental implications. Environ. Res. 192, 110326.

Fang, C., Zheng, R., Zhang, Y., Hong, F., Mu, J., Chen, M., Song, P., Lin, L., Lin, H., Le, F., Bo, J., 2018. Microplastic contamination in benthic organisms from the Arctic and sub-Arctic regions. Chemosphere 209, 298–306.

Ferreira, G.V.B., Barletta, M., Lima, A.R.A., Morley, S.A., Justino, A.K.S., Costa, M.F., 2018. High intake rates of microplastics in a Western Atlantic predatory fish, and insights of a direct fishery effect. Environ. Pollut. 236, 706–717.

Forster, C.E., Norcross, B.L., Mueter, F.J., Logerwell, E.A., Seitz, A.C., 2020. Spatial patterns, environmental correlates, and potential seasonal migration triangle of polar cod (Boreogadus saida) distribution in the Chukchi and Beaufort seas. Polar Biol. 43, 1073–1094.

Galloway, T.S., Cole, M., Lewis, C., 2017. Interactions of microplastic debris throughout the marine ecosystem. Nat. Ecol. Evol. 1, 116.

Goldstein, M.C., Rosenberg, M., Cheng, L.N., 2012. Increased oceanic microplastic debris enhances oviposition in an endemic pelagic insect. Biol. Lett. 8, 817–820.

González-Pleiter, M., Velázquez, D., Edo, C., Carretero, O., Gago, J., Barón-Sola, Á., Hernández, L.E., Yousef, I., Quesada, A., Leganés, F., Rosal, R., Fernández-Piñas, F., 2020. Fibers spreading worldwide: microplastics and other anthropogenic litter in an Arctic freshwater lake. Sci. Total Environ. 722, 137904.

Halsband, C., Herzke, D., 2019. Plastic litter in the European Arctic: what do we know? Emerg. Contam. 5, 308–318.

Holmes, R.M., Coe, M.T., Fiske, G.J., Gurtovaya, T., McClelland, J.W., Shiklomanov, A.I., Spencer, R.G., Tank, S.E., Zhulidov, A.V., 2013. Climate change impacts on the hydrology and biogeochemistry of Arctic rivers. In: Goldman, C.R., Kumagai, M., Robarts, R.D. (Eds.), Climatic Change and Global Warming of Inland Waters: Impacts and Mitigation for Ecosystems and Societies. John Wiley, Hoboken, N. J., pp. 3–26.

Huntington, A., Corcoran, P.L., Jantunen, L.M., Thaysen, C., Bernstein, S., Stern, G.A., Rochman, C.M., 2020. A first assessment of microplastics and other anthropogenic particles in Hudson Bay and the surrounding eastern Canadian Arctic waters of Nunavut. Facets 5, 432–454.

Isobe, A., Iwasaki, S., Uchida, K., Tokai, T., 2019. Abundance of non-conservative microplastics in the upper ocean from 1957 to 2066. Nat. Commun. 10, 417.

Jiang, Y., Yang, F., Zhao, Y., Wang, J., 2020. Greenland Sea Gyre increases microplastic pollution in the surface waters of the Nordic seas. Sci. Total Environ. 712, 136484.

Kane, I.A., Clare, M.A., Miramontes, E., Wogelius, R., Rothwell, J.J., Garreau, P., Pohl, F., 2020. Seafloor microplastic hotspots controlled by deep-sea circulation. Science 368, 1140–1145.

Kanhai, D.K., Gardfeldt, K., Krumpen, T., Thompson, R.C., O'Connor, I., 2020. Microplastics in sea ice and seawater beneath ice floes from the Arctic Ocean. Sci. Rep. 10, 5004.

Kanhai, D.K., Gårdfeldt, K., Lyashevska, O., Hassellöv, M., Thompson, R.C., O'Connor, I., 2018. Microplastics in sub-surface waters of the Arctic Central Basin. Mar. Pollut. Bull. 130, 8–18.

Kanhai, K., Johansson, C., Frias, J.P.G.L., Gardfeldt, K., Thompson, R.C., O'Connor, I., 2019. Deep sea sediments of the Arctic Central Basin: a potential sink for microplastics. Deep-Sea Res. I Oceanogr. Res. Pap. 145, 137–142.

Kim, S.-K., Lee, H.-J., Kim, J.-S., Kang, S.-H., Yang, E.-J., Cho, K.-H., Tian, Z., Andrady, A., 2021. Importance of seasonal sea ice in the western Arctic Ocean to the Arctic and global microplastic budgets. J. Hazard. Mater. 418, 125971.

Knutsen, H., Cyvin, J.B., Totland, C., Lilleeng, Ø., Wade, E.J., Castro, V., Pettersen, A., Laugesen, J., Møskeland, T., Arp, H.P.H., 2020. Microplastic accumulation by tube-dwelling, suspension feeding polychaetes from the sediment surface: a case study from the Norwegian Continental Shelf. Mar. Environ. Res. 161, 105073.

Lebreton, L., Egger, M., Slat, B., 2019. A global mass budget for positively buoyant macroplastic debris in the ocean. Sci. Rep. 9, 12922.

Lebreton, L.C.M., van der Zwet, J., Damsteeg, J.W., Slat, B., Andrady, A., Reisser, J., 2017. River plastic emissions to the world's oceans. Nat. Commun. 8, 15611.

Lilleeng, Ø., 2018. The Presence of Microplastics on the Norwegian Continental Shelf and in Rio Almendares, Havana. Norwegian University of Life Sciences, Norway.

Lima, A.R.A., Ferreira, G.V.B., Barrows, A.P.W., Christiansen, K.S., Treinish, G., Toshack, M.C., 2021. Global patterns for the spatial distribution of floating microfibers: Arctic Ocean as a potential accumulation zone. J. Hazard. Mater. 403, 123796.

Lin, H., Wang, J., Liu, K., He, X., Lin, J., Huang, Y., Zhang, S., Mou, J., Zheng, C., Wang, Y., 2016. Benthic macrofaunal production for a typical shelf–slope–basin region in the western Arctic Ocean. Cont. Shelf Res. 113, 30–37.

Liu, K., Wu, T., Wang, X., Song, Z., Zong, C., Wei, N., Li, D., 2019. Consistent transport of terrestrial microplastics to the ocean through atmosphere. Environ. Sci. Technol. 53, 10612–10619.

Lots, F.A.E., Behrens, P., Vijver, M.G., Horton, A.A., Bosker, T., 2017. A large-scale investigation of microplastic contamination: abundance and characteristics of microplastics in european beach sediment. Mar. Pollut. Bull. 123, 219–226.

Lusher, A.L., Burke, A., O'Connor, I., Officer, R., 2014. Microplastic pollution in the Northeast Atlantic Ocean: validated and opportunistic sampling. Mar. Pollut. Bull. 88, 325–333.

Lusher, A.L., Tirelli, V., O'Connor, I., Officer, R., 2015. Microplastics in Arctic polar waters: the first reported values of particles in surface and sub-surface samples. Sci. Rep. 5, 1–9.

Marineregions.org, 2016. Towards a standard for georeferenced marine names. Chukchi Plateau. https://www.marineregions.org/gazetteer.php?p=details&id=7806.

Morgana, S., Ghigliotti, L., Estévez-Calvar, N., Stifanese, R., Wieckzorek, A., Doyle, T., Christiansen, J.S., Faimali, M., Garaventa, F., 2018. Microplastics in the Arctic: a case study with sub-surface water and fish samples off Northeast Greenland. Environ. Pollut. 242, 1078–1086.

Møskeland, T., Knutsen, H., Arp, H.P., Lilleeng, Ø., Pettersen, A., 2018. Microplastics in Sediments on the Norwegian Continental Shelf.

Mu, J., Qu, L., Jin, F., Zhang, S., Fang, C., Ma, X., Zhang, W., Huo, C., Cong, Y., Wang, J., 2019a. Abundance and distribution of microplastics in the surface sediments from the northern Bering and Chukchi seas. Environ. Pollut. 245, 122–130.

Mu, J., Zhang, S., Qu, L., Jin, F., Fang, C., Ma, X., Zhang, W., Wang, J., 2019b. Microplastics abundance and characteristics in surface waters from the Northwest Pacific, the Bering Sea, and the Chukchi Sea. Mar. Pollut. Bull. 143, 58–65.

National Snow and Ice Data Center, 2021. Sea ice index: Arctic- and Antarctic-wide changes in sea ice. https://nsidc.org/data/seaice_index/bist.

Obbard, R.W., Sadri, S., Wong, Y.Q., Khitun, A.A., Baker, I., Thompson, R.C., 2014. Global warming releases microplastic legacy frozen in Arctic Sea ice. Earth's Future 2, 315–320.

Onink, V., Wichmann, D., Delandmeter, P., van Sebille, E., 2019. The role of Ekman Currents, Geostrophy, and Stokes Drift in the accumulation of floating microplastic. J. Geophys. Res. Oceans 124, 1474–1490.

PAME, 2019. Desktop study on marine litter including microplastics in the Arctic. Arctic Marine Litter Entry and Dispersion Pathways. 11th Arctic Council Ministerial Meeting, Rovaniemi, Finland. 29.

Peeken, I., Bergmann, M., Gerdts, G., Katlein, C., Krumpen, T., Primpke, S., Tekman, M., 2018a. Microplastics in the Marine Realms of the Arctic with special emphasis on sea ice. Arctic Report Card 2018. 88.

Peeken, I., Primpke, S., Beyer, B., Gütermann, J., Katlein, C., Krumpen, T., Bergmann, M., Hehemann, L., Gerdts, G., 2018b. Arctic Sea ice is an important temporal sink and means of transport for microplastic. Nat. Commun. 9, 1505.

Ross, P.S., Chastain, S., Vassilenko, E., Etemadifar, A., Zimmermann, S., Quesnel, S.A., Eert, J., Solomon, E., Patankar, S., Posacka, A.M., Williams, B., 2021. Pervasive distribution of polyester fibres in the Arctic Ocean is driven by Atlantic inputs. Nat. Commun. 12, 106.

Scheringer, M., Wegmann, F., Fenner, K., Hungerbühler, K., 2000. Investigation of the cold condensation of persistent organic pollutants with a global multimedia fate model. Environ. Sci. Technol. 34, 1842–1850.

Stroeve, J., Notz, D., 2018. Changing state of Arctic sea ice across all seasons. Environ. Res. Lett. 13, 103001.

Sundet, J.H., Herzke, D., Jenssen, M., 2016. Forekomst og kilder av mikroplastikk i sediment, og konsekvenser for bunnlevende fisk og evertebrater på Svalbard. Sluttrapport, Svalbards Miljøvernfond, RIS prosjekt 10495.

Sundet, J.H., Herzke, D., Jenssen, M., 2017. Forekomst av mikroplastikk i sjøvann, bunnsedimenter, fjaeresediment og i filtrerende bunnorganismer i naere kystområder på Svalbard. In: Miljøvernfond, S. (Ed.), Sluttrapport. Syselmannen, Norway, pp. 1–10.

Tekman, M.B., Wekerle, C., Lorenz, C., Primpke, S., Hasemann, C., Gerdts, G., Bergmann, M., 2020. Tying up loose ends of microplastic pollution in the Arctic: distribution from the sea surface through the water column to deep-sea sediments at the HAUSGARTEN Observatory. Environ. Sci. Technol. 54, 4079–4090.

Thomas, S., Manju Lekshmi, N., 2017. Recent trends in fishing gear materials. In: Ravishankar, C.N., Prasad, M.M., Mohanty, A.K., Murugadas, V., ManjuLekshmi, N., Anandan, R., Sajeev, M.V., Mohan, C.O., Rejula, K., Aniesrani Delfiya, D.S. (Eds.), Recent Trends in Harvest and Post-harvest Technologies in Fisheries. Central Institute of Fisheries Technology, Kochi, India. ICAR-Central Institute of Fisheries Technology.

Van Sebille, E., Wilcox, C., Lebreton, L., Maximenko, N., Hardesty, B.D., Van Franeker, J.A., Eriksen, M., Siegel, D., Galgani, F., Law, K.L., 2015. A global inventory of small floating plastic debris. Environ. Res. Lett. 10, 124006.

von Friesen, L.W., Granberg, M.E., Pavlova, O., Magnusson, K., Hassellov, M., Gabrielsen, G.W., 2020. Summer sea ice melt and wastewater are important local sources of microlitter to Svalbard waters. Environ. Int. 139, 105511.

Whitmire, S.L., Van Bloem, S.J., 2017. Quantification of Microplastics on National Park Beaches. NOAA Marine Debris Program. National Oceanic and Atmospheric Administration.

Wilson, R.R., Perham, C., French-McCay, D.P., Balouskus, R., 2018. Potential impacts of offshore oil spills on polar bears in the Chukchi Sea. Environ. Pollut. 235, 652–659.

Woodall, L.C., Sanchez-Vidal, A., Canals, M., Paterson, G.L., Coppock, R., Sleight, V., Calafat, A., Rogers, A.D., Narayanaswamy, B.E., Thompson, R.C., 2014. The deep sea is a major sink for microplastic debris. R. Soc. Open Sci. 1, 140317.

Woodgate, R., 2013. Arctic Ocean circulation: going around at the top of the world. Nat. Educ. Knowl. 4, 1–15.

Xiong, B., Loss, R.D., Shields, D., Pawlik, T., Hochreiter, R., Zydney, A.L., Kumar, M., 2018. Polyacrylamide degradation and its implications in environmental systems. npj Clean Water 1, 17.

Yakushev, E., Gebruk, A., Osadchiev, A., Pakhomova, S., Lusher, A., Berezina, A., van Bavel, B., Vorozheikina, E., Chernykh, D., Kolbasova, G., 2021. Microplastics distribution in the Eurasian Arctic is affected by Atlantic waters and Siberian rivers. Commun. Earth Environ. 2, 1–10.

Zeng, J., Chen, M., Zheng, M., Hu, W., Qiu, Y., 2017. A potential nitrogen sink discovered in the oxygenated Chukchi Shelf waters of the Arctic. Geochem. Trans. 18, 1–15.

Zhang, J., Lindsay, R., Schweiger, A., Steele, M., 2013. The impact of an intense summer cyclone on 2012 Arctic sea ice retreat. Geophys. Res. Lett. 40, 720–726.

Zhang, B., Wu, D., Yang, X., Teng, J., Liu, Y., Zhang, C., Zhao, J., Yin, X., You, L., Liu, Y., Wang, Q., 2019. Microplastic pollution in the surface sediments collected from Sishili Bay, North Yellow Sea, China. Mar. Pollut. Bull. 141, 9–15.

Zhao, J., Ran, W., Teng, J., Liu, Y., Liu, H., Yin, X., Cao, R., Wang, Q., 2018a. Microplastic pollution in sediments from the Bohai Sea and the Yellow Sea, China. Sci. Total Environ. 640–641, 637–645.

Zhao, S., Ward, J.E., Danley, M., Mincer, T.J., 2018b. Field-based evidence for microplastic in marine aggregates and mussels: implications for trophic transfer. Environ. Sci. Technol. 52, 11038–11048.